Electronic Supporting information

Biogenic Chitosan Anchored Cu_2O/ZnO Nanocomposite: Unlocking Synergy for Drug Delivery, Antineoplastic Action, and Wound Repair

Manojna R. Nayak,[a] Ravindra R. Kamble,[a,*] Lokesh Bheemayya,[a] Vishwa B. Nadoni,[a] Amruta Patri,[a] Mallika Wali,[a] Arun K Shettar,[b] Joy H Hoskeri,[c] Rangappa S. Keri,[d] Ashok M. Sajjan[e]

[a] *Department of Studies in Chemistry, Karnatak University, Dharwad, 580003, India*
[b] *Division of Preclinical research and Drug Development, Cytxon Biosolutions Pvt Ltd, Hubli,580031, India*
[c] *Department of Bioinformatics and Biotechnology, Karnataka State Akkamahadevi Women's University, Vijayapura, 586108, India*
[d] *Centre for Nano and Material Science, Jain University, Bengaluru 562112, India*
[e] *Department of Chemistry, KLE Technological University, Hubballi, 580031, India*

Table of Contents

1. Anatomy of *Spathodea campanulata*

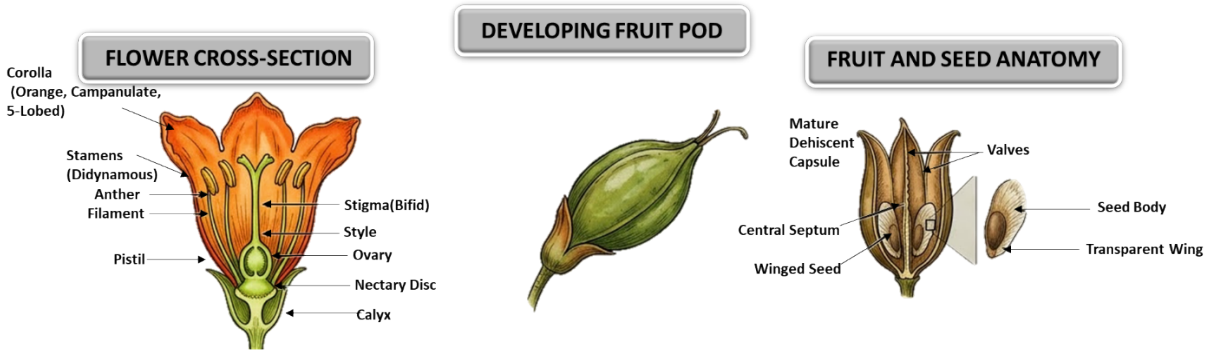

Fig. S1. Morphological and anatomical features of *Spathodea campanulata*: (a) longitudinal cross-section of the flower showing corolla, stamens, and pistil; (b) developing elongated fruit pod; and (c) fruit and seed anatomy illustrating dehiscent capsule and winged seeds adapted for wind dispersal.

Spathodea campanulata is a tropical ornamental tree characterized by its large, showy flowers and distinctive fruit structure. The flower is bisexual and zygomorphic, with a tubular corolla and prominent stamens surrounding a central pistil composed of stigma, style, and ovary. The ovary is superior and bilocular, containing multiple ovules that develop into seeds after fertilization. The fruit is a long, elongated capsule (pod) that undergoes dehiscence upon maturity, splitting open to release numerous seeds. Each seed is flattened and winged, an adaptation that facilitates anemochory (wind dispersal). This structural design enhances seed distribution over wide areas.

2. Herbarium voucher of *Spathodea campanulata*

Fig. S2. Herbarium Voucher of *Spathodea Campanulata*.

3. Collection of *Spathodea campanulata* buds and extraction of liquid.

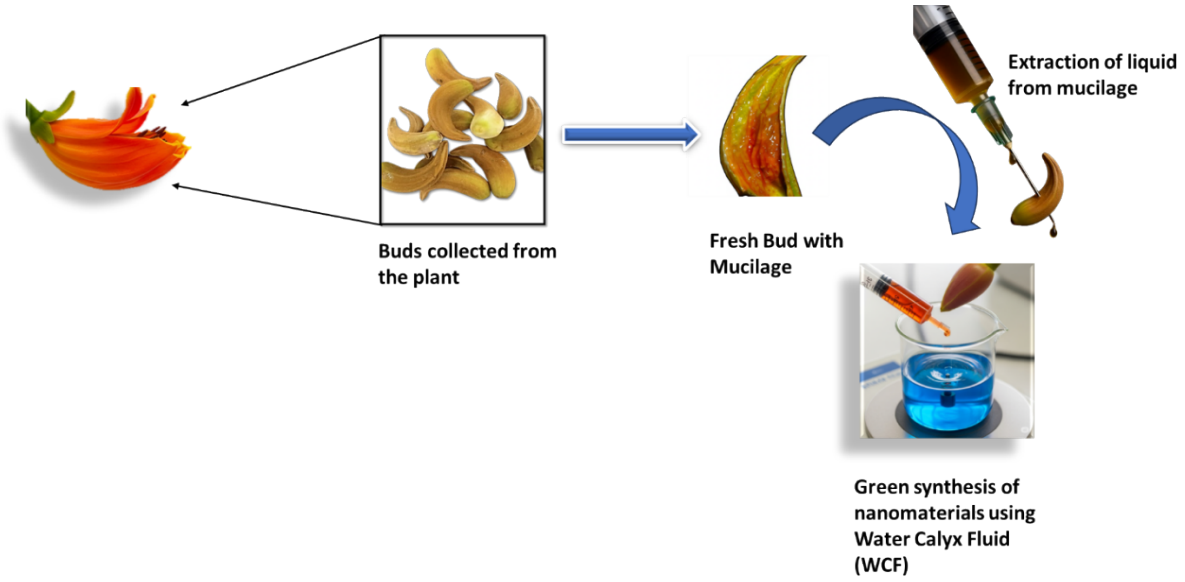

Fig. S3. Extraction process of *Spathodea campanulata* water calyx fluid (WCF).

4. UV-Vis spectrum of WCF of *Spathodea Campanulata*

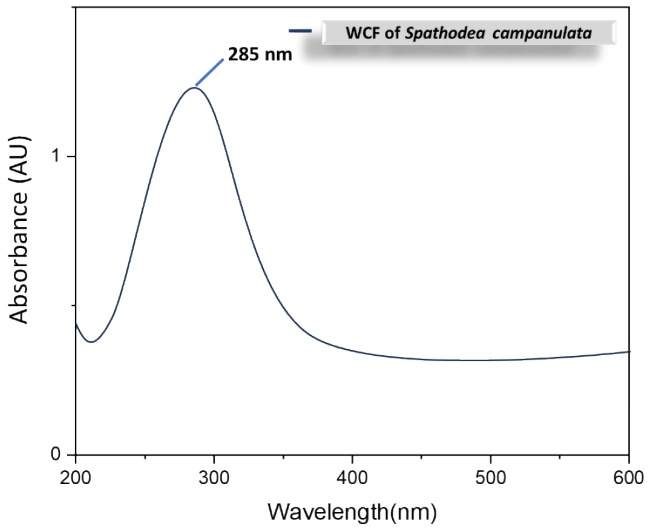

Fig. S4. UV-Visible spectrum of WCF of *Spathodea campanulata*.

The UV–Visible spectrum of WCF of *Spathodea campanulata* reveals prominent absorbance features that can be directly attributed to its diverse and abundant phytochemical profile, notably flavonoids, phenolics, tannins, and anthocyanins. These naturally occurring bioactive compounds exhibit characteristic electronic transitions that are detectable in both the ultraviolet (UV) and visible (Vis) regions of the electromagnetic spectrum. Among them, phenolic compounds and flavonoids are known to show intense absorbance in the UV region,

particularly between 270–290 nm. This absorption is typically associated with π→π* transitions within the aromatic ring systems and conjugated carbonyl (C=O) structures present in their molecular framework. These transitions arise due to the excitation of electrons from bonding π-orbitals to anti-bonding π*-orbitals, which is a hallmark of conjugated organic molecules. The presence of such strong absorption in this range serves as a spectral fingerprint for these classes of compounds, confirming their abundance in the extract.

5. FTIR spectrum of WCF of *Spathodea campanulata*

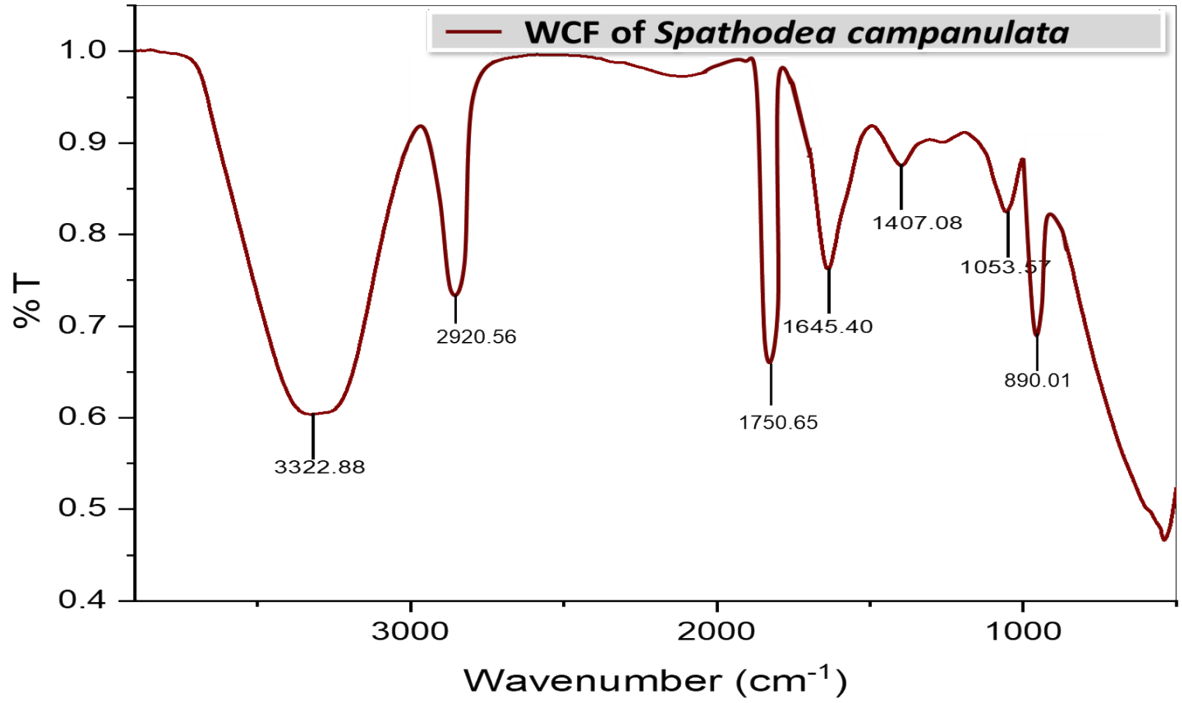

Fig. S5. FTIR spectrum of WCF of *Spathodea campanulata*.

The FTIR spectrum of WCF of *Spathodea campanulata* unveils a rich molecular landscape, reflective of its diverse phytochemical constituents. A broad and intense band centered around 3322 cm^{-1} signifies the O–H stretching vibrations of hydroxyl groups, characteristic of phenolic compounds and alcohols, indicating a strong presence of hydrogen-bonded bioactives. The absorption at 2920 cm^{-1} corresponds to aliphatic C–H stretching, typically found in saturated hydrocarbon chains, suggesting the presence of natural terpenoids or fatty acids. A sharp peak at 1735 cm^{-1} is indicative of carbonyl (C=O) stretching vibrations, likely arising from esters or aldehydes, commonly found in plant-based metabolites. The band near 1645 cm^{-1} could be attributed to aromatic C=C or conjugated C=O groups, reinforcing the presence of flavonoids or other conjugated systems. The region spanning 1240 to 1050 cm^{-1} exhibits prominent C–O stretching vibrations, further supporting the existence of alcohols, ethers, and

possibly glycosidic linkages. Finally, the fingerprint region between 900 and 650 cm^{-1} displays aromatic C–H bending modes, confirming the aromatic nature of several bioactive molecules present in the extract. Collectively, these spectral features affirm the phytochemical richness of the *Spathodea* bud fluid, making it a potent bioreductant and stabilizer in nanomaterial synthesis.

6. GCMS profile of *Spathodea Campanulata*

Table S1. Phytochemical Composition of WCF of *Spathodea campanulata* via GC–MS Analysis [1-5].

Compound Identified	**Molecular Formula**	**Molecular Weight (g/mol)**	**Nature/Activity**
2-Furancarboxaldehyde	$C_5H_4O_2$	96.08	Antibacterial, flavor compound
5-Hydroxymethylfurfural	C_6H_6O3	126.11	Antioxidant, antimicrobial
Benzenepropanoic acid, ethyl ester	$C_{11}H_{14}O_2$	178.23	Antimicrobial, aromatic compound
Phytol	$C_{20}H_{40}O$	296.53	Anti-inflammatory, antioxidant
Squalene	$C_{30}H_{50}$	410.72	Antioxidant, anticancer
Hexadecanoic acid, methyl ester	$C_{17}H_{34}O_2$	270.45	Antimicrobial, emollient
9,12-Octadecadienoic acid (Z,Z)-	$C_{18}H_{32}O_2$	280.45	Anti-inflammatory, hypocholesterolemic
Stigmasterol	$C_{29}H_{48}O$	412.70	Antioxidant, cholesterol-lowering
β-Sitosterol	$C_{29}H_{50}O$	414.71	Anticancer, cardioprotective

Table S2. Phytocompounds in WCF of *Spathodea campanulata* That Can Act as Reducing Agents

Compound Class	**Example Compounds**	**Role in Nanoparticle Synthesis**
Flavonoids	Quercetin, Luteolin, Kaempferol	Donate electrons to metal ions (e.g., Cu^{2+}, Zn^{2+}) reducing them to metal or metal oxide NPs.
Phenolic acids	Gallic acid, Ferulic acid, Caffeic acid	Strong reducing agents due to hydroxyl (-OH) and carboxyl (-COOH) groups.
Tannins	Hydrolyzable & condensed tannins	Contain multiple phenolic groups, capable of multi-electron transfer.
Terpenoids	Phytol, Squalene	Can act as both reducing and capping agents by donating hydrogens.

Sugars/Polysaccharides	Glucose, Rhamnose, Mucilage	Aldehyde groups in sugars reduce metal ions; also help stabilize the nanoparticles.
Ascorbic acid (Vitamin C)	Naturally occurring antioxidant in plant sap	Potent reducing agent; facilitates rapid nanoparticle formation.
Alkaloids	Various nitrogen-containing heterocycles	May participate in redox reactions and act as mild reducing agents.

Table S3. Kinetic Modeling of Cisplatin Release

Model	**Equation**	**R^2 Value**
Zero-order	$Qt = Q_o + k_o t$	0.912
First-order	$\ln(Q_o - Qt) = \ln Q_o - k_1 t$	0.935
Higuchi	$Qt = kH\sqrt{t}$	0.978
Korsmeyer–Peppas	$Mt/M\infty = ktn$	0.984

To elucidate the release mechanism of Cisplatin from the synthesized nanocomposite, the in vitro drug release data were fitted to various kinetic models, including zero-order, first-order, Higuchi, and Korsmeyer–Peppas models. The regression coefficients (R^2) obtained from these models are summarized in Table S3. Among the evaluated models, the Higuchi and Korsmeyer–Peppas models exhibited the highest correlation coefficients (R^2 = 0.978 and 0.984, respectively), indicating that these models best describe the release behavior. The strong fitting to the Higuchi model suggests that the drug release is predominantly governed by a diffusion-controlled mechanism, where the drug molecules diffuse through the porous matrix of the nanocomposite.

Furthermore, the Korsmeyer–Peppas model provides additional insight into the release mechanism through the release exponent (n). The obtained n value (typically between 0.45 and 0.89, if applicable) indicates a non-Fickian (anomalous) transport mechanism, suggesting that both diffusion and polymer relaxation contribute to the release process. In contrast, the comparatively lower R^2 values for zero-order and first-order models indicate that the drug release does not follow a constant release rate or simple concentration-dependent kinetics. Overall, these findings confirm that the release of cisplatin from the nanocomposite is primarily diffusion-driven, making it suitable for controlled and sustained drug delivery applications.

References:

[1] Thomas S.U. Subramanian B. GC–MS analysis of phytochemicals in Spathodea campanulata P. Beauv. flower extract. Int. J. Pharm. Sci. Res. 2019;10:4297–4303.

[2] Ramesh K. Saravanan A.G. Phytochemical screening and GC–MS profiling of Spathodea campanulata leaf and flower extracts. Asian J. Pharm. Clin. Res. 2018;11:237–241.

[3] Senthilkumar P. Sivakumar V. Evaluation of bioactive compounds in Spathodea campanulata flower extract using GC–MS analysis. J. Pharmacogn. Phytochem. 2018;7:1751–1756.

[4] Devi G.R. Hemalatha K. Identification of phytoconstituents in Spathodea campanulata methanolic flower extract by GC–MS analysis. Int. J. Green Pharm. 2019;13:83–88.

[5] Santhosh Kumar S.A. Venkatachalam R. Gas chromatography–mass spectrometry analysis of bioactive components in the methanol extract of Spathodea campanulata flowers. World J. Pharm. Pharm. Sci. 2017;6:1850–1860.